Fuel 92 (2012) 37–48

Contents lists available at ScienceDirect

Fuel

journal homepage: www.elsevier.com/locate/fuel

Real-time and robust estimation of biodiesel blends

Saleh Mirheidari [a,*], Matthew Franchek [a], Karolos Grigoriadis [a], Javad Mohammadpour [a], Yue-Yun Wang [b], Ibrahim Haskara [b]

[a] Department of Mechanical Engineering University of Houston, Houston, TX 77204, United States
[b] Propulsion Systems Research Lab, General Motors Company, Warren, MI 48090, United States

ARTICLE INFO

Article history:
Received 24 January 2011
Received in revised form 4 May 2011
Accepted 29 June 2011
Available online 27 July 2011

Keywords:
Fuel blend estimation
System Identification
Online adaptive model

ABSTRACT

Biodiesel as a renewable alternative fuel produces lower exhaust emissions with the exception of nitrogen oxides (NO_x) when compared to the conventional diesel fuel. Reducing nitrogen oxides produced from engines running on biodiesel requires proper engine controller adaptations that are linked to the specifics of the fuel blend. Therefore, online estimation of fuel blend is a critical step in allowing diesel engines to maintain performance while simultaneously meeting emission requirements when operating on biodiesel blends. Presented in this paper are three different model-based biodiesel blend estimation strategies using: (i) crankshaft torsionals, (ii) NO_x emissions measurement from the exhaust stream, and (iii) oxygen content measurement of the exhaust stream using a wide-band UEGO sensor. Each approach is investigated in terms of the accuracy and robustness to sensor errors. A sensitivity analysis is conducted for each method to quantify robustness of the proposed fuel blend estimation methods.

1. Introduction

Although diverse in composition, biodiesel fuels are generally characterized as having long chain alkyl esters synthesized from the transesterification of vegetable oils thus producing an oxygenated renewable fuel. These fuels can be used directly in diesel engines in their pure biomass form or as a blended fuel containing biomass and hydrocarbon-based diesel. Therefore, biodiesel is a candidate fuel substitute for the existing vast diesel engine fleet [1].

The production of biodiesel is achieved through the conversion of triglycerides fats to ester via transesterification with methanol or ethanol. Two-stage low-temperature transesterification and solvent-free reaction systems are the standard methods for biodiesel production [2]. In general, vegetable oil contains 97% of triglycerides and 3% of di- and mono-glycerides and fatty acids. The process of removal of all glycerol and the fatty acids from the vegetable oil in the presence of a catalyst is called "transesterification". The vegetable oil reacts with methanol and forms esterified vegetable oil in the presence of sodium/potassium hydroxide which is the catalyst of choice [1]. Different biodiesel fuels have differing physical and chemical properties, such as viscosity and heating value. At present, soy oil is the dominant feedstock; however, numerous other seed oils have been investigated – including canola, sunflower, cottonseed, palm, and jatropha, to name a few. In addition, some biodiesel synthesis is focusing on recycling by using animal fats and waste cooking oils as feedstock [4]. Beyond vegetable oils, rapeseed oil is the most important source of the biodiesel in Europe [5]. Most recently, the use of algae oil has been developing as a source of biodiesel production [6]. Algae oil is feasible as a source of biodiesel in the United States but the associated production cost is high thus limiting its commercial viability.

Biodiesels have been studied from combustion, performance and emission points of view in a growing number of investigations [7,2,8]. Biodiesel is usually in a blend with petroleum-based diesel because of the benefits of conventional diesel due to its viscosity. The notation used to represent different biodiesel blend fuels is a letter "*B*" followed by a number, which indicates the percentage of biodiesel. For instance, *B*0 is conventional diesel, *B*20 contains 20% biodiesel, and *B*100 is pure biodiesel. In the following section, different aspects of biodiesel properties including combustion, performance and emission are reviewed.

In various independent studies, biodiesel combustion characteristics have been investigated [9]. In general, there are combustion and emission trends that are common to all biomass fuels when compared to conventional diesel. The leading commonality is lower in-cylinder pressure for biodiesel fuels. Owing to the lower energy content of biodiesel, the heating value is reduced and the released energy becomes lower. Therefore, the in-cylinder pressure is lower for biodiesel and its associated blends.

Another combustion parameter is the heat release rate, which is an indicator of the released energy. The heat release rate for a given percentage of biodiesel in blend is lower compared to its petroleum counterpart. This is a consequence of the shorter ignition delay thus reducing the premix combustion phase for biomass. In

* Corresponding author.
E-mail address: smirheidari@uh.edu (S. Mirheidari).

0016-2361/$ - see front matter © 2011 Elsevier Ltd. All rights reserved.
doi:10.1016/j.fuel.2011.06.060

comparison, conventional diesel fuels increase the accumulation of fuel during the relatively longer delay period resulting in a higher rate of heat release. Biodiesel has normally a higher cetane number compared to petroleum-based diesel. The higher the cetane number the less the ignition delay is. Therefore, biodiesel leads to a shorter ignition delay compared to conventional diesel. Due to shorter ignition delay of biodiesel, the maximum heat release occurs earlier compared to diesel. Performance parameters such as output power, fuel consumption and thermal efficiency are paramount when evaluating biodiesel fuels. The produced power by biodiesel has been reported to be slightly less compared to hydrocarbon diesel [1,10]. Ozsezen et al. [11] reported that when the test engine was fueled with waste palm oil methyl ester and canola oil methyl ester, the maximum engine torque reduced slightly while the brake specific fuel consumption (BSFC) increased compared to petroleum-based diesel fuels. This downward trend in maximum brake torque and upward trend in the BSFC are indeed due to the lower energy content of the biodiesel. In biodiesel usage a higher amount of fuel is consumed to achieve similar maximum brake torque causing an increase in the BSFC.

In various research studies, fuel consumption of biodiesel has been reported to vary significantly. For example, using palm oil and canola oil in a study by Ozsezen et al. [11], an increase in fuel consumption was shown when compared to conventional diesel. An experimental investigation on a vehicle has been conducted by Ropkins et al. [12], which shows that the fuel consumption of a 1.8 L diesel engine running on *B*5 biodiesel is 7–8% higher compared to diesel engine.

Biodiesel usage has a direct impact on tailpipe emissions. Specifically, carbon monoxide (CO), unburned hydrocarbons (HC) and particulate matters (PM) decrease by about 50%, 50% and 65% on average, respectively [13]. In spite of all these environmental benefits, there is an average increase of about 10% in NO_x production [14,15]. Approaches to NO_x reduction have been proposed using exhaust gas recirculation (EGR) technology [33] or adding chemicals to biodiesel fuel. Because of this increase in NO_x, there is a need to accurately estimate, in real-time, the biocontent of the fuel so that the on-board engine controller can appropriately adapt the engine operation after each tank refill to mitigate this negative effect.

Biomass content can be estimated based on the change in the chemical properties of biofuels using commercial sensors. To this purpose, refraction or dielectric sensors (fuel composition sensor) [3], infrared (NIR) spectroscopy or nuclear magnetic resonance (NMR) sensors [30], and ultraviolet (UV) absorption spectroscopy sensors [31] are available. In ultraviolet spectroscopy sensor method, the absorbance of the fuel for different biodiesel blends has a linear relation with the blend level in some specific wavelength ranges. Therefore, for those specific waves, the absorbance can determine the blend level [31]. In fuel composition sensors, the sensor output frequency shifts as the amount of biocontent increases. There is about 14% change in the output frequency when fuels are switched from diesel to biodiesel. This frequency shift leads to biodiesel blend estimation with less than 10% error [3]. Biocontent sensing has also been proposed using information from a wideband oxygen sensor in the engine exhaust [16]. Since biomass fuels are oxygenated fuels, there is a measureable increase in the oxygen atoms in the exhaust stream [16]. Experimental results for steady-state estimation of biodiesel blend using such a sensor demonstrated an average 4% error.

The above biomass fuel estimation methods and concepts require the introduction of a new sensor. Adding such a new sensor increases the engine production and maintenance cost and adds diagnostics requirements. The inclusion of a new sensor also introduces robustness issues with regards to ambient environmental changes and reliability challenges.

Presented in this manuscript are three new fuel blend estimation methods using various sensor measurements. The first approach utilizes the produced torque from the engine as manifested in the crankshaft torsionals. The fundamental principle driving the proposed method is the difference between the energy content of conventional diesel and biodiesel fuels. The advantage of this approach over other methods in the literature is that it can be accomplished using existing sensors mounted on a diesel engine. The second proposed estimation method is based on the NO_x emissions produced by the engine. This method utilizes the difference between the NO_x emissions from biodiesel and diesel along with some other information such as fuel flow. The last proposed approach is the use of a wide-band oxygen sensor for biodiesel blend estimation. The basic principle for this approach is the difference between the oxygen content of biodiesel and diesel, and the fact that 10% of biodiesel weight is oxygen while diesel does not have any oxygen in its composition. All three approaches will be studied in terms of their robustness and estimation sensitivity.

The organization of the paper is as follows: Section 2 introduces the engine simulation model used to validate the biocontent estimation approaches. In Section 3, the three proposed biodiesel blend estimation methods are described and the robustness of each method is analyzed against uncertainty and measurement error. In Section 4, the proposed biodiesel estimation methods are compared and validated in a detailed engine simulation environment.

2. Diesel engine model and biodiesel fuel library

To validate the proposed estimation strategies, a biodiesel combustion numerical model is employed. In this section, the diesel engine model used for validation of the estimation strategies is detailed followed by a presentation of the biofuel library developed. A 6-cylinder diesel engine model is developed in GT-Power software which is a widely used software tool in engine and combustion simulation [17]. GT-Power does not include biodiesel in its fuel library. Therefore, the biodiesel and its blends must be defined in the software using different chemical and physical properties of the fuel or blend.

2.1. Diesel engine model

The model for the validation of the biocontent estimation approaches is developed in GT-Power [17]. A 6-cylinder diesel engine model is developed to predict the performance of the designed estimators. Table 1 contains the specifications of the engine model.

The developed GT-Power model is combined with a proportional integral (PI) controller in MATLAB for engine speed control. The torque load on the engine is considered as an unknown disturbance input. Engine speed is not the only monitored parameter of the engine model; it is, however, the regulated engine output. The other engine parameters monitored through GT-Power include exhaust emissions and combustion parameters. To quantify the model predictions, in-cylinder pressure and instantaneous engine speed of the diesel engine model are shown in Figs. 1 and 2, respectively [17].

Table 1
6-Cylinder diesel engine model specifications.

Engine type	Diesel
Displacement	6.7 L
Injection type	Direct injection
No. of cylinders	6

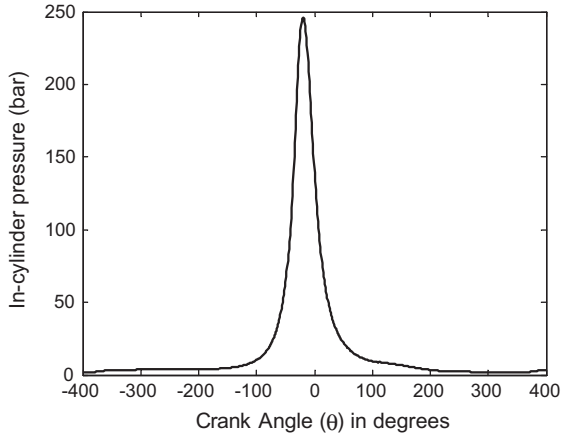

Fig. 1. In-cylinder pressure for engine model at 1600 rpm and 400 ft.lb.

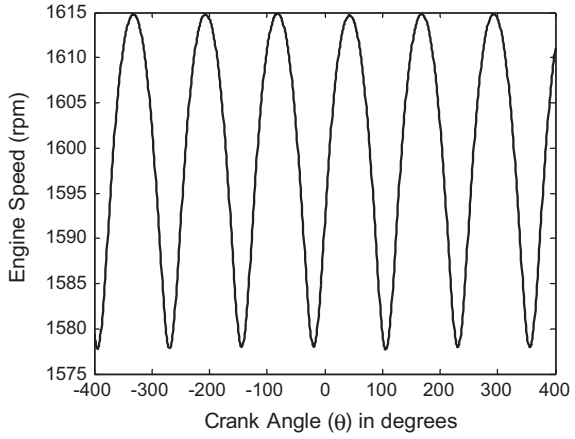

Fig. 2. Instantaneous engine speed signal for diesel engine model at 1600 rpm and 400 ft.lb.

Table 2
Biodiesel fuel properties.

Property	Soybean biodiesel	Unit
Heat of vaporization at 298°K	357	kJ/kg
Density at 298°K	890.7	kg/m^3
Number of carbon atoms in each molecule	18.82	–
Number of oxygen atoms in each molecule	2	–
Number of hydrogen atoms in each molecule	34.39	–
Lower heating value of the fuel	37.11	MJ/kg
Critical temperature	785.87	K
Critical pressure	12.07	bar
Dynamic viscosity at 300°K	4.5×10^{-6}	kg/(m s)

2.2. Development of the biodiesel fuel library in GT-Power

The fuel library in GT-Power includes the specifications of the fuel properties [18], among which are viscosity, surface tension, density, and heat of vaporization of the fuel. Some of the physical properties are difficult to quantify, for example enthalpy. Dynamic viscosity and thermal conductivity are two properties established for different temperatures. Listed in Table 2 are the properties used to create a soybean biodiesel fuel library in GT-Power [18]. Also shown in Figs. 3 and 4 are the thermal conductivity and viscosity for the soybean-based biodiesel fuel as a function of temperature and fuel state.

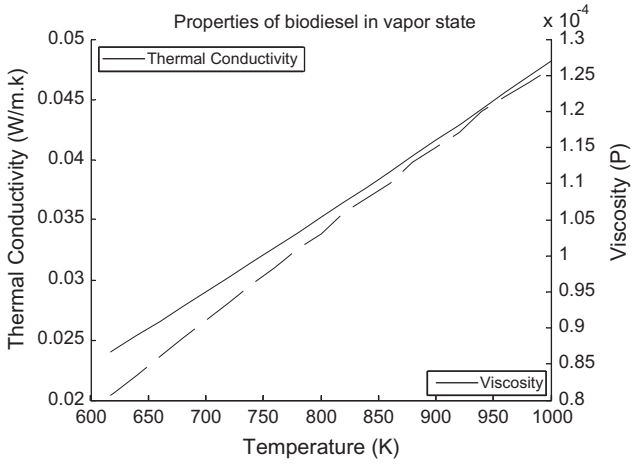

Fig. 3. Thermal conductivity and viscosity of soybean biodiesel in vapor state.

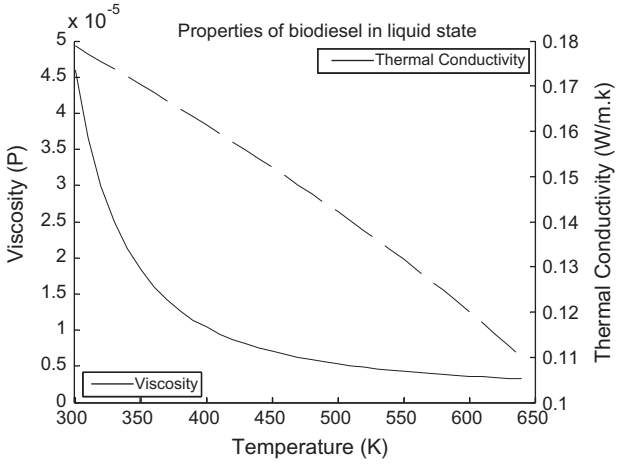

Fig. 4. Thermal conductivity (left) and viscosity (right) of soybean biodiesel in liquid state.

3. Proposed approaches for biodiesel content estimation

In this section, three solutions to real-time biodiesel blend estimation are described. The methods are based on the fundamentals of combustion physics and chemistry combined with the sensor information. In particular, when using biodiesel as an engine fuel there are consistent changes in the power produced and the resulting emissions. These changes will be exploited in the proposed methods for biomass content estimation.

3.1. Estimation using crankshaft torsionals information

The energy content of biodiesel is almost 12% less than that of the conventional diesel fuel. This difference leads to a reduction in torque production from the engine since the energy release of the fuel is converted to mechanical torque. This difference between produced torque of the hydrocarbon diesel fuel and biodiesel fuel can be exploited for biomass content estimation provided that engine torque can be estimated. Concerning the torque estimation, the crankshaft torsionals due to the engine firing event can be employed [19]. This estimation method is based on the fact that the crankshaft twist during a power stroke is directly related to the engine brake torque. However, instead of estimating the torque as in [19], the twist of the crankshaft during a power stroke will be

directly used in our approach. Combing the crankshaft twist with nominal engine speed and the mass of fueling command from the engine control enables the biomass content estimation.

3.1.1. Theoretical background

The relation between produced power and torque in an internal combustion engine is

$$P = 2\pi NT \tag{1}$$

where P is engine power (in kW), N is engine rotational speed (in rev/s) and T is the produced torque (in N m) [20]. The power in (1) is called *brake power*. A measure of fuel efficiency is the *fuel conversion efficiency* η_f defined by

$$\eta_f = \frac{P}{\dot{m}_f Q_{HV}} \tag{2}$$

where $\dot{m}_f$ is fuel rate injected per cycle (in kg/s) and Q_{HV} is the heating value of the fuel (in kJ/kg). This efficiency measure is determined in a standardized test procedure in which a known mass of fuel is fully burned with air, and the thermal energy released by the combustion process is absorbed by a calorimeter as the combustion products cool down to their original temperature [20]. From (1) and (2)

$$Q_{HV} = \frac{2\pi}{\eta_f}\frac{NT}{\dot{m}_f} \tag{3}$$

which indicates the relationship between heating value of the fuel and a combination of torque and fuel consumption.

Based on the difference between the heating values of the diesel fuel and biodiesel, a linear relation exists between the heating value of the blend and the percentage of biodiesel [32], namely

$$BD = aQ_{HV} + b \tag{4}$$

where a and b are constants determined from the experiments. From (3) and (4), the following relationship is obtained

$$BD = a\frac{2\pi}{\eta_f}\frac{NT}{\dot{m}_f} + \mathrm{b} \tag{5}$$

A real-time brake torque estimation strategy has been proposed in [19] where the instantaneous measured engine speed serves as the model input to the torque estimation algorithm. The model is comprised of notch filters executed in the crank angle domain to extract mean engine speed and the n-th frequency component from the instantaneous engine speed signal in real-time (n denotes the number of cylinders). The investigated approach for a 6-cylinder engine has shown that the brake torque of the engine can be estimated using engine speed N and M_6 (the magnitude of the engine speed signal at the engine firing frequency). This value (M_6) has information on crankshaft torsionals that will be used later. For conventional diesel fuel

$$T = f(N, M_6) \tag{6}$$

where $f(.)$ is a nonlinear function identified in [19]. In the biomass fuel case the torque is a function of engine speed N, M_6 and biodiesel blend content (BD).

By substituting (6) into (5), we have

$$BD = a\frac{2\pi}{\eta_f}\frac{Nf(BD, N, M_6)}{\dot{m}_f} + \mathrm{b} \tag{7}$$

Finally, assuming that the fuel conversion efficiency η_f is almost constant for different biodiesel blends [29,8], the biodiesel blend would be

$$BD = \mathrm{function}(N, M_6, \dot{m}_f) \tag{8}$$

Therefore, the proposed biocontent fuel estimator will have three inputs. The preliminary results for this estimator are shown in [21]. However, the robustness of this method and its sensitivity to measurement errors in N, M_6 and $\dot{m}_f$ were not investigated in [21]. Hence, a robust estimation methodology paralleling the method in [21] is investigated in this paper.

3.1.2. Description of a robust estimation methodology

The proposed biodiesel blend estimation will utilize the engine control fueling command, the engine speed and the filtered engine speed signal (M_6). However, there is a robustness issue that must be investigated due to unavoidable errors in the sensor measurements and fueling commands from ECU. To compensate for these errors, an information synthesis approach is proposed in [22]. This approach results in an online adaptive model whose parameters depend on the fuel type in the combustion chamber. This model can be calibrated using collected data from the engine along with the use of physics-based relations. To illustrate this approach, assume that the following equation represents the mentioned model

$$y = c_1 f_1(x_1, \ldots, x_n) + c_2 f_2(x_1, \ldots, x_n) + c_3 f_3(x_1, \ldots, x_n) \tag{9}$$

where y is the output and $x_1, \ldots, x_n$ are the inputs of the model. The f_i's are the regressors of the model and c_i's are the coefficients. The approach is to compare the output of the model with the actual measurement from the engine and adapt the coefficients (c_i's) based on the error vector $E = y - \tilde{y}$ (where $\tilde{y}$ is the measured signal). For the nominal system, the coefficients are ($c_{1n}\ c_{2n}\ c_{3n}$) and the difference between the set of online estimated model coefficients and the set of nominal model coefficients results in a parameter variation vector represented by $(\Delta c_1\ \Delta c_2\ \Delta c_3)^T$. The model structure and result are shown in Figs. 5 and 6, respectively. In Fig. 6, the parameter variation vector for the nominal model is the null vector, but in case of any discrepancy or model mismatch with the nominal model, there would be a non-zero vector as shown in Fig. 6. For biodiesel blend estimation, the nominal system is considered to be the model corresponding to the conventional diesel. Any biodiesel blend in the fuel leads to a non-zero parameter variation vector due to a change in the coefficients of the model. As observed later, the length of this non-zero parameter variation vector determines the percentage of the biodiesel blend.

An important part in the estimator design is to determine a model that leads to a robust estimation. Diesel engine physics integrated with system identification tools will address the robustness concerns. To derive the online adaptive model structure, we start with (2) and we have

$$T = \frac{\overbrace{\eta_f Q_{HV}\dot{m}_{f\max}}^{\tilde{a}}}{2\pi N_{max}}\frac{\dot{m}_f}{\tilde{N}} = \tilde{a}\frac{\dot{m}_f}{\tilde{N}} \tag{10}$$

There are two new terms which appear when normalizing both fuel flow rate and engine speed, denoted by $\dot{\tilde{m}}_f$ and $\tilde{N}$. To obtain the Taylor series expansion of the term $\frac{1}{\tilde{N}}$, rewrite (10) as follows

$$T = \frac{\tilde{a}\dot{\tilde{m}}_f 1}{1 - (1 - \tilde{N})} \tag{11}$$

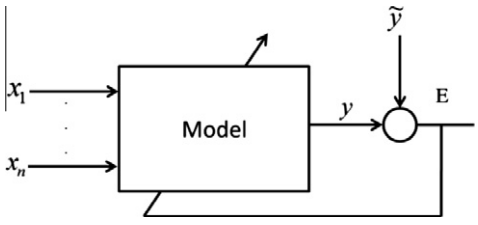

Fig. 5. Model with adaptive coefficients.

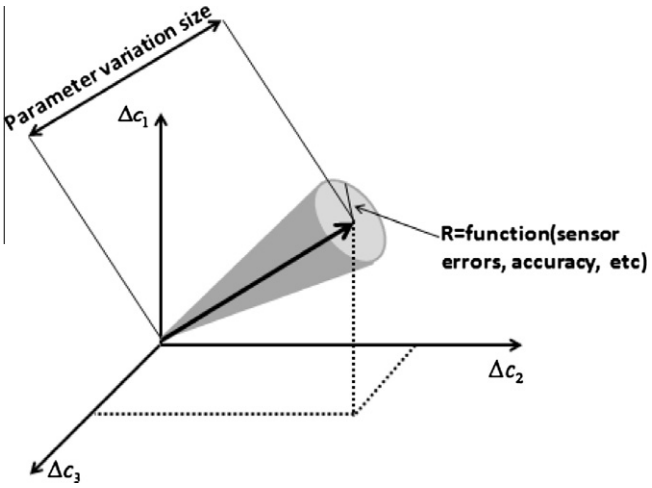

Fig. 6. Biodiesel blend estimation using parameter variation vector synthesis.

Now from the Taylor series expansion and using normalized engine parameters gives

$$T = \tilde{a}\dot{\tilde{m}}_f\left(2 - \tilde{N} + \frac{(1-\tilde{N})^2}{2!} + \frac{(1-\tilde{N})^3}{3!} + \cdots\right) \tag{12}$$

Consider the first two terms of the Taylor series expansion in (12) while neglecting the higher order terms. The result is

$$T = \tilde{a}\dot{\tilde{m}}_f(2 - \tilde{N}) \tag{13}$$

and

$$T = 2\tilde{a}\dot{\tilde{m}}_f - \tilde{a}\dot{\tilde{m}}_f\tilde{N} \tag{14}$$

In [19], it is shown that the M_6 component is related to the torque. That is,

$$M_6 \propto T = 2\tilde{a}\dot{\tilde{m}}_f - \tilde{a}\dot{\tilde{m}}_f\tilde{N} \tag{15}$$

The simplest case relating M_6 with (14) is to consider M_6 as an indicator of the torque. Then

$$M_6 \approx c_1\dot{\tilde{m}}_f + c_2\dot{\tilde{m}}_f\tilde{N} \tag{16}$$

Now, to shift the data around the origin in the multi-dimensional space of operation, a bias term is added to (16). This bias term can compensate for the effects of ignored higher order terms in Taylor series as well. The result is

$$M_6 \approx c_1\dot{\tilde{m}}_f + c_2\dot{\tilde{m}}_f\tilde{N} + c_3 \tag{17}$$

The block diagram of the estimation approach is shown in Fig. 7 where the inputs to the model are fueling rate and average engine speed signal and the output is the crankshaft torsionals which is an indicator of produced brake torque of the engine. Eq. (17) is valid in steady-state conditions and the coefficients carry information on the heating value of the fuel that we seek to determine the biodiesel blend.

Using collected data from the diesel engine model, the identified coefficients c_i for different biodiesel blends enable a biomass content estimate. For this purpose, an engine running at a different torque and speed operating point, the steady-state values for all the required measurements are collected and used to adapt the model coefficients. The load profile that has been used for running the engine model in GT-Power is shown in Fig. 8. This profile is used for several engine speeds, and the steady-state data is collected for adaptation of the model (17). The three parameters $(c_1\ c_2\ c_3)^T$ form a vector for each specific blend. The blends used in this

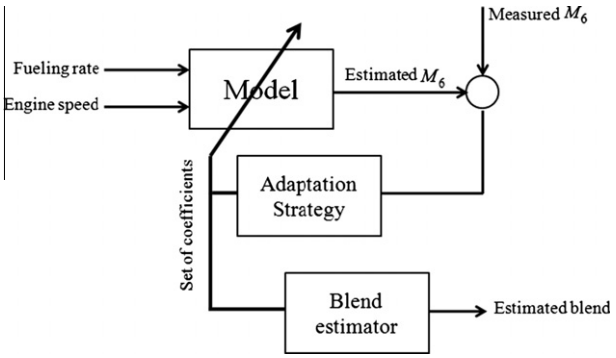

Fig. 7. Block diagram of the proposed robust estimation strategy.

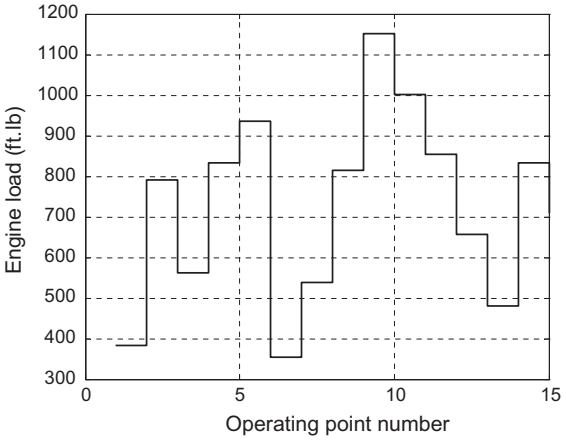

Fig. 8. Engine load profile for running the engine model in GT-Power.

paper are *B*0, *B*20, *B*50, and *B*100. We choose the vector of the coefficients for *B*0 blend to be the reference (nominal) coefficients vector, and any vector is compared to the reference vector. Assume the reference vector is $\left(c^{TF}_{1,B0}c^{TF}_{2,B0}c^{TF}_{3,B0}\right)^T$, then

$$(\Delta c_1 \quad \Delta c_2 \quad \Delta c_3\ )^T = \left(\frac{c^{TF}_{1,B0} - c_1}{c^{TF}_{1,B0}}\ \frac{c^{TF}_{2,B0} - c_2}{c^{TF}_{2,B0}}\ \frac{c^{TF}_{3,B0} - c_3}{c^{TF}_{3,B0}}\right)^T \tag{18}$$

where $(\Delta c_1\ \Delta c_2\ \Delta c_3)^T$ is called the parameter variation vector (the variation from coefficients corresponding to *B*0 is calculated for

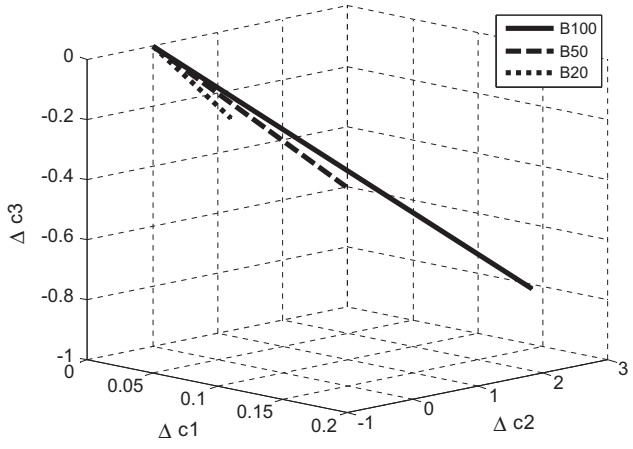

Fig. 9. Parameter variation vectors for different biodiesel blends for estimated M_6 component.

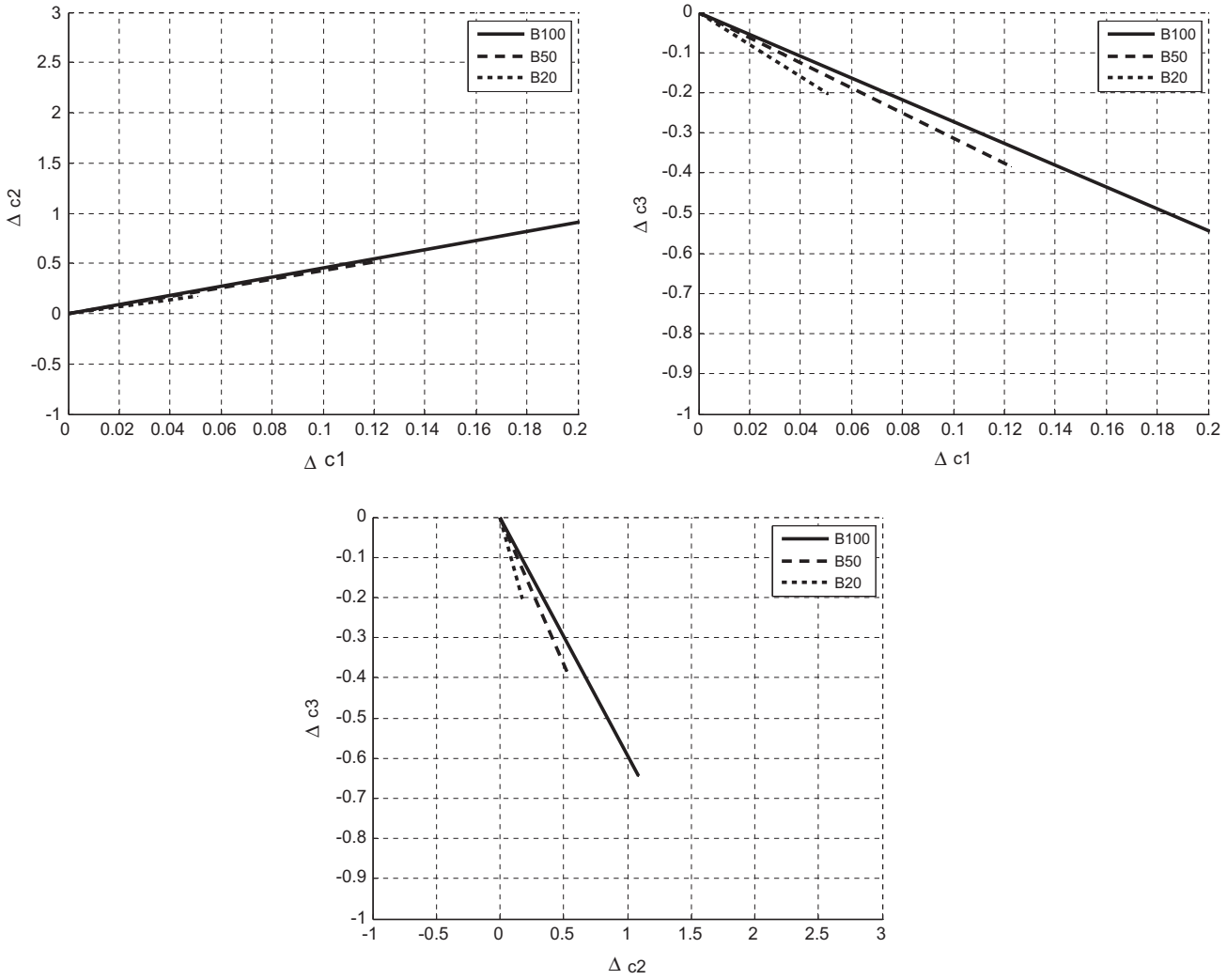

Fig. 10. Vectors from the difference between the coefficients of the model and the reference coefficients projected on different axes.

every blend), and the superscript *TF* stands for the crankshaft torsionals and fuel method.

The vector $(\Delta c_1\ \Delta c_2\ \Delta c_3)^T$ is shown in Fig. 9 for different biodiesel blends. The solid line vector in this figure is related to *B*100, the dashed line to *B*50, and the dotted line to *B*20. Clearly for the reference vector *B*0, $(\Delta c_1\ \Delta c_2\ \Delta c_3)^T = (0\ 0\ 0)^T$ when neglecting measurement uncertainty. Therefore, the $(\Delta c_1\ \Delta c_2\ \Delta c_3)$ vector in Fig. 9 for *B*0 is a dot at the origin in case of no error or uncertainty in the inputs of the estimator. However, there will be a non-zero vector corresponding to *B*0 when input uncertainties are present. The plot in Fig. 9 is shown again in Fig. 10 from different angles in different 2D planes.

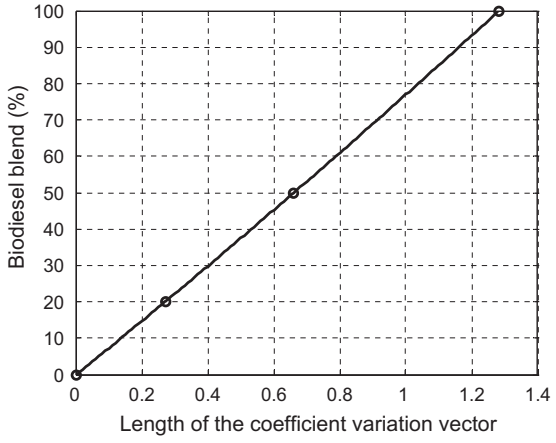

Fig. 11. Length of the projected vector on the reference vector vs. biodiesel blend.

Designing the blend estimator using the length of the parameter variation vector leads to the following equation for the biodiesel blend estimate

$$BD = 77.83L \tag{19}$$

where *BD* is biodiesel blend percentage and *L* is the length of the parameter variation vector. Shown in Fig. 11 is the plot of (19) compared to actual blends. In this figure, the circle points are the actual blends and the line is fitted to this data.

3.1.3. Sensitivity analysis

This section details the sensitivity analysis for the designed biodiesel blend estimator. The fact that measurement errors and noises are inevitable requires a sensitivity analysis of any designed estimation algorithm whose inputs are sensor measurements. In the designed estimator in (19), *L* is determined by

$$L = \sqrt{\left(\frac{c^{TF}_{1,B0} - c_1}{c^{TF}_{1,B0}}\right)^2 + \left(\frac{c^{TF}_{2,B0} - c_2}{c^{TF}_{2,B0}}\right)^2 + \left(\frac{c^{TF}_{3,B0} - c_3}{c^{TF}_{3,B0}}\right)^2} \tag{20}$$

where $c_i's$ are the parameters from the model in (17) and $c^{TF\prime}_{i,B0}s$ are the reference parameters that correspond to $B0$. Substituting (20) into (19) gives

$$BD = 77.83\sqrt{\left(\frac{c^{TF}_{1,B0}-c_1}{c^{TF}_{1,B0}}\right)^2+\left(\frac{c^{TF}_{2,B0}-c_2}{c^{TF}_{2,B0}}\right)^2+\left(\frac{c^{TF}_{3,B0}-c_3}{c^{TF}_{3,B0}}\right)^2} \quad (21)$$

Now uncertainties are considered to be as in the multiplicative form. The uncertainties in the measurements are as follows

$$\dot{\hat{m}} = r\dot{m}_f \quad (22)$$

$$\widehat{M}_6 = sM_6 \quad (23)$$

$$\widehat{N} = kN \quad (24)$$

The measurement errors appear directly in the model parameters in (17). Hence, the measurement errors affect the parameter estimates. For instance, 3% error in fueling rate measurement translates to 3% change in c_1 which is the coefficient of $\dot{m}_f$ and 3% change in c_2 which is the coefficient of $\dot{m}_f N$. Therefore, any error in fueling rate measurement leads to error in c_1, c_2, and any error in average engine speed measurement affects c_2, However, any error in the 6th component changes all the parameters because

$$sM_6 \approx sc_1\dot{m}_f + sc_2\dot{m}_f N + sc_3 \quad (25)$$

To check the sensitivity of the designed estimator, the variation of the function (21) due to the variation in the coefficients is evaluated. This can be done using partial differentiation. The estimated biodiesel blend (BD) variation for any of the coefficients would be

$$\frac{\partial BD}{\partial c_1} = \frac{-2\times\frac{77.83}{c^{TF}_{1,B0}}\left(\frac{c^{TF}_{1,B0}-c_1}{c^{TF}_{1,B0}}\right)}{L} \quad (26)$$

$$\frac{\partial BD}{\partial c_2} = \frac{-2\times\frac{77.83}{c^{TF}_{2,B0}}\left(\frac{c^{TF}_{2,B0}-c_2}{c^{TF}_{2,B0}}\right)}{L} \quad (27)$$

$$\frac{\partial BD}{\partial c_3} = \frac{-2\times\frac{77.83}{c^{TF}_{3,B0}}\left(\frac{c^{TF}_{3,B0}-c_3}{c^{TF}_{3,B0}}\right)}{L} \quad (28)$$

The Eqs. (26)–(28) indicate the variation of BD for any changes in $c_i's$ For instance, if the actual blend is $B50$ and we had 3% error in $\dot{m}_f$ and 5% error in engine speed measurements, we would have 0.12% error in BD estimation because

$$\left.\frac{\partial BD}{\partial c_1}\right|_{B50} = \frac{-2\times\frac{77.83}{c^{TF}_{1,B0}}\left(\frac{c^{TF}_{1,B0}-c_{1,50}}{c^{TF}_{1,B0}}\right)}{L_{B50}} = -31.92 \quad (29)$$

$$\left.\frac{\partial BD}{\partial c_2}\right|_{B50} = \frac{-2\times\frac{77.83}{c^{TF}_{2,B0}}\left(\frac{c^{TF}_{2,B0}-c_{2,50}}{c^{TF}_{2,B0}}\right)}{L_{B50}} = 2165.9 \quad (30)$$

$$\left.\frac{\partial BD}{\partial c_3}\right|_{B50} = \frac{-2\times\frac{77.83}{c^{TF}_{3,B0}}\left(\frac{c^{TF}_{3,B0}-c_{3,50}}{c^{TF}_{3,B0}}\right)}{L_{B50}} = 828.8 \quad (31)$$

where L_{B50} is the length of parameter variation vector for $B50$, and the variation of estimated BD is calculated as follows

$$\Delta BD = \Delta c_{1,50}\times\left.\frac{\partial BD}{\partial c_1}\right|_{B50} + \Delta c_{2,50}\times\left.\frac{\partial BD}{\partial c_2}\right|_{B50} + \Delta c_{3,50}\times\left.\frac{\partial BD}{\partial c_3}\right|_{B50} \quad (32)$$

where $\Delta c_{1.50}$, $\Delta c_{2.50}$, $\Delta c_{3.50}$ and are the coefficient variations in presence of the measurement errors. Hence, the biodiesel blend estimation error is

$$\begin{aligned}\Delta BD &= -\Delta c_{1,50}\times 31.92 + \Delta c_{2,50}\times 2165.9 + \Delta c_{3,50}\times 828.8\\ &= -4\% \end{aligned} \quad (33)$$

Therefore the estimated BD would be within 0.1160 of the actual blend, which is $B50$ in the presence of mentioned measurement errors. This value is less than 4% of the actual blend ($B50$). This example shows that the approach is robust to additive and multiplicative measurement errors. Assuming that there is an error in M_6 component, it will lead to a small error in BD estimation as well.

3.2. Biodiesel blend estimation using NO_x sensor

In this section, the goal is to develop a biodiesel blend estimator using a NO_x emissions sensor. A NO_x sensor is typically a high temperature device built to detect nitrogen oxides in combustion environments such as an automobile or truck tailpipe. The drive to develop a NO_x sensor comes from environmental factors. NO_x gases can cause various problems such as smog and acid rain. Many governments around the world have passed laws to limit their emissions along with other combustion gases such as SO_x (oxides of sulfur), CO (carbon monoxide), CO_2 (carbon dioxide) and hydrocarbons. One way of minimizing NO_x emissions is to first detect the levels in an exhaust stream and then employ combustion control to minimize NO_x production [23]. A significant amount of work has appeared detailing the sensitivity and accuracy of the NO_x sensors [24–26]. Today there exist commercialized NO_x sensors in the market.

Presented in this section is a method of biodiesel blend estimation using NO_x information measured from a NO_x sensor. The difference between biodiesel and diesel NO_x emissions is the basic principle for the proposed method. NO_x emissions produced from the biodiesel fuels are normally higher than those from diesel fuels with the amounts contingent upon the biomass content and engine type. The NO_x emissions from biodiesel are typically 10% higher than that of the conventional diesel. The increase can go up to 23% for some biodiesel fuels [7]. The reasons for the increase in NO_x emissions are still unknown, but there are some explanations that have been provided in the literature [7]. Fuel oxygen content is believed to be one of the reasons since existence of more oxygen in the cylinder can result in a higher temperature, which leads to higher NO_x emissions. This higher NO_x production of biodiesel is the basic principle for this section. Using a NO_x sensor to measure the NO_x emissions in the exhaust path along with some readings from ECU can provide information for biodiesel blend estimation.

3.2.1. Theoretical background

To estimate the biodiesel blend using a NO_x sensor, we utilize the same adaptive method as in the last section. The relationship for nitrogen oxide formation rate is [20]:

$$\frac{d[NO]}{dt} = \frac{6\times10^{16}}{\sqrt{T}}e^{\frac{-69090}{T}}\sqrt{[O_2]_e}[N_2]_e \quad (34)$$

where [.] denotes species concentration in moles per cubic centimeter [20] and $[.]_\varepsilon$ is [.] at the equilibrium. Define the function

$$f_T(T) = \frac{6\times10^{16}}{\sqrt{T}}e^{\frac{-69090}{T}} \quad (35)$$

Then from (34) and (35)

$$\frac{d[NO]}{dt} = f_T(T)\sqrt{[O_2]_e[N_2]_e} \quad (36)$$

From the above equation, $\frac{d[NO]}{dt}$ can be rewritten as a function of $\sqrt{[O_2]_\theta}$ and $[N_2]_\theta$. Hence

$$\frac{d[NO]}{dt} \approx g\left(\sqrt{[O_2]_e}, [N_2]_e\right) \quad (37)$$

where the effect of the temperature T appears in the nonlinear function g. Define a function h such that

$$g\left(\sqrt{[O_2]_e}, [N_2]_e\right) = \frac{dh\left(\sqrt{[O_2]_e}, [N_2]_e\right)}{dt} \tag{38}$$

Hence

$$[NO] \approx h\left(\sqrt{[O_2]_e}, [N_2]_e\right) + constant \tag{39}$$

Based on the fact that biodiesel is an oxygenated fuel while conventional diesel fuel is not, the source of oxygen in the combustion chamber is both fuel and air. On the other hand, the nitrogen source is just air assuming that the fuels are nitrogen-free or have very small nitrogen content. Finally, $\sqrt{[O_2]_\theta}$ and $[N_2]_\theta$ can be replaced by fuel and air rate to the combustion chamber. Hence

$$[NO] \approx \tilde{h}(\dot{m}_f, \dot{m}_a) + constant \tag{40}$$

where $\dot{m}_f$ is the fuel rate and $\dot{m}_a$ is air rate to the combustion chamber and $\tilde{h}$ is a scalar function. Moreover, we know that

$$AFR = \frac{\dot{m}_a}{\dot{m}_f} \tag{41}$$

Therefore, from (40) and (41)

$$[NO] \approx \dot{h}(\dot{m}_f, AFR.\dot{m}_f) + constant \tag{42}$$

Any nonlinear function $\tilde{h}$ can be approximated by first two terms of its Taylor series expansion

$$[NO] \approx c_1\dot{m}_f + c_2 AFR.\dot{m}_f + c_3 \tag{43}$$

The collected data from diesel engine model in GT-Power are used to validate the model (43). The data generated from the GT-Power model is used to identify the best model structure, which turns out to be exactly the same structure as in (43). The output of the model in (43) is compared to the actual output from the diesel engine model. The results are shown in Fig. 12. As can be seen, the estimated NO is consistent with the actual NO from the diesel engine model. Thus, an online adaptive biomass estimation model using information provided by NO_x sensor measurement, AFR and $\dot{m}_f$ will be developed.

3.2.2. Adaptive estimation strategy

As described in Section 3.2.1, NO_x sensor measurement, AFR and $\dot{m}_f$ can be used for biodiesel blend estimation. The same estimator structure as in Fig. 7 is used here with different inputs and output. The inputs to the model are AFR and $\dot{m}_f$ and the output is NO_x sensor measurement. Using recursive least-squares (RLS) method for the adaptation of the model coefficients (c_i's in (43)) the parameter variation vectors for different biodiesel blends are shown in Figs. 13 and 14. By evaluating the vectors with existence of the measurement errors, it is determined that changes in the third coefficient (c_3) are not significant. The reason is that the NO_x emission of biodiesel is different from petroleum-based diesel fuel and it leads to different bias terms for [NO] model. The final adaptive biomass estimator model is

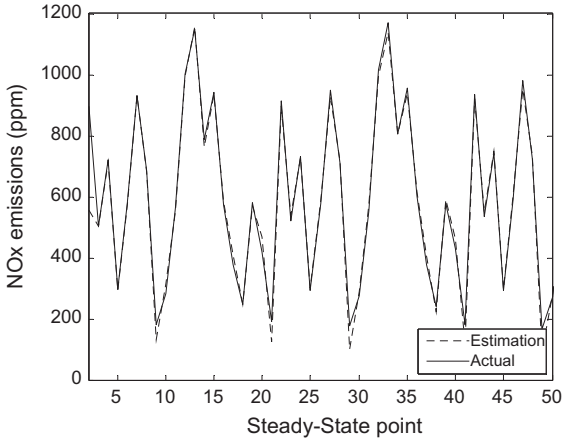

Fig. 12. NO estimation (for blend $B50$) using $\{\dot{m}_f, \dot{m}_f.AFR, 1\}$ as the regressors.

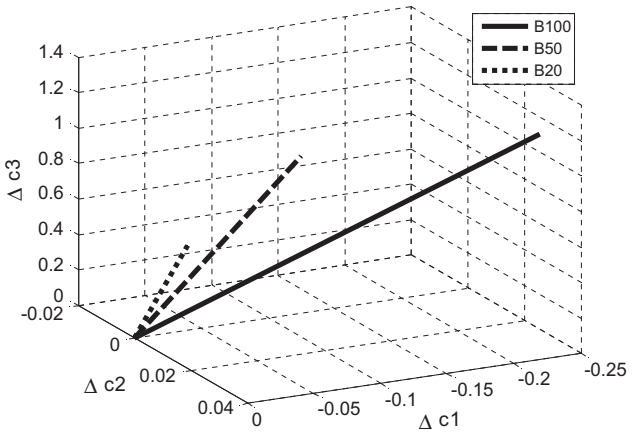

Fig. 13. Parameter variation vectors for different biodiesel blends for NO_x formation in 3D.

$$BD = 77.87\left(c^{NO}_{3,B0} - c_3\right)^2 - 97.6\left(c^{NO}_{3,B0} - c_3\right) \tag{44}$$

where $c^{NO}_{i,B0}$'s are the coefficients of the model (43) for $B0$. The estimator is based on only the third coefficient of the model (43). The sensitivity analysis is developed in the next section for this estimator. The parameter variation vectors for the estimator in (44) are shown in Fig. 15, where the circles indicate the measured points.

3.2.3. Sensitivity analysis

Similar to Section 3.1.3, the impact of NO_x sensor error on biodiesel blend estimation is investigated. The designed estimator in (44) only depends on c_3. In this case, we only need to analyze the estimation error with respect to the errors that affect c_3. As mentioned before, the only change that affects c_3 is error in the NO_x sensor measurements. Assuming that there is a multiplicative error s in the NO_x measurement,

$$s[NO] = sc_1\dot{m}_f + sc_2 AFR.\dot{m}_f + sc_3 \tag{45}$$

In (45), the multiplicative error of NO appears in the bias term of the model. Any other error in reading and measurements will not affect the bias term.

Now similar to Section 3.1.3 the sensitivity of the estimator (44) respect to c_3 is as follows

$$\frac{dBD}{dc_3} = -2 \times 77.87\left(c^{NO}_{3,B0} - c_3\right) - 97.6 \tag{46}$$

We assume that there is a 5% error in NO_x measurement (when the fuel blend is $B50$). Then the deviated bias term would be $\frac{c_3}{1.05} = -0.191$. Therefore, the variation of the BD estimation resulting from NO_x sensor error will be

$$\left.\frac{\partial BD}{\partial c_3}\right|_{B50} = -2 \times 77.87\left(c^{NO}_{3,B0} - c_{3,50}\right) - 97.6 = -37.06 \tag{47}$$

$$\Delta BD = \Delta c_{3,50} \times \left.\frac{\partial BD}{\partial c_3}\right|_{B50} = 0.01 \times -37.06 = -0.35 \tag{48}$$

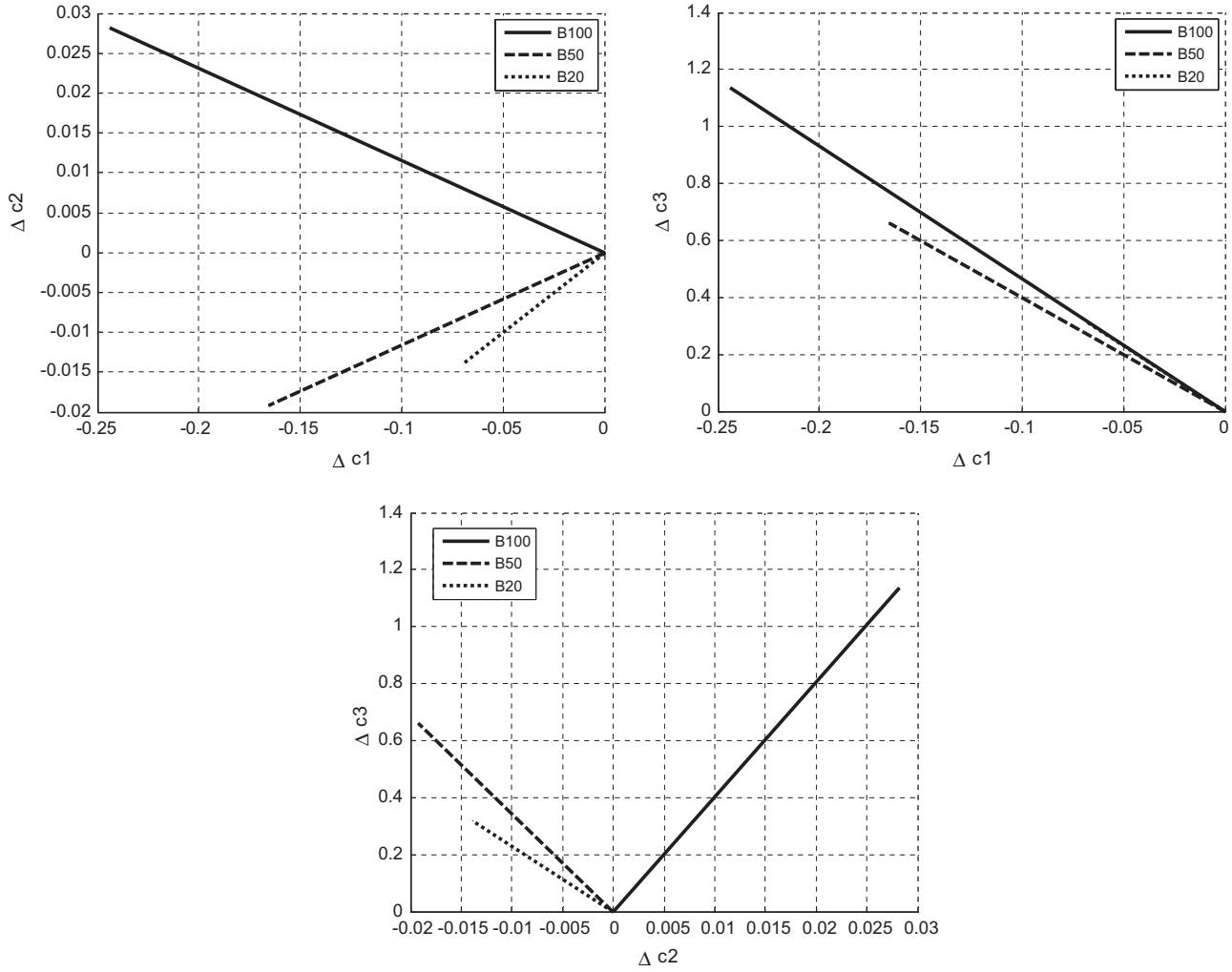

Fig. 14. Parameter variation vectors for different biodiesel blends for $\mathbf{NO_x}$ formation in 2D.

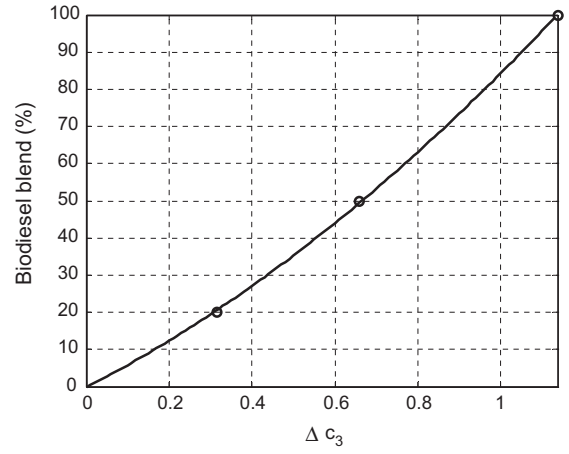

Fig. 15. Biodiesel blend vs. the third coefficient variation (Δc_3).

Therefore, the error in biodiesel blend estimation for *B*50 with existence of 5% error in NO_x measurement will be −0.35%.

3.3. Biodiesel blend estimation using UEGO sensor

A universal exhaust gas oxygen (UEGO) sensor is utilized in this part of the work for the purpose of biodiesel blend estimation. The fact that biodiesel is an oxygenated fuel is the fundamental basis for this approach. Since biodiesel and petroleum-based diesel fuel have similar composition except for oxygen existence in biodiesel, the oxygen flow in the exhaust would be higher for biodiesel combustion compared to the conventional diesel. Steady-state biodiesel blend estimation has been achieved by Snyder et al. [16]. In this paper, we use the derived model in [16] to develop an adaptive biodiesel blend estimation strategy similar to the previous sections. The advantage of this work compared to others is its real-time implementation capability.

3.3.1. Theoretical model and estimator design

In this section, the development of an online adaptive biomass estimation model for the adaptive method using UEGO sensor is described. The global reaction of a generic oxygenated hydrocarbon fuel ($C_nH_mO_r$) with idealized air ($O_2 + \varepsilon N_2$) to major products is

$$\begin{aligned} &C_nH_mO_r + \lambda\left(n+\frac{m}{4}-\frac{r}{2}\right)(O_2+N_2) \\ &\quad\rightarrow nCO_2+\frac{m}{2}H_2O+(\lambda-1)\times\left(n+\frac{m}{4}-\frac{r}{2}\right)O_2 \\ &\qquad+\lambda\epsilon\left(n+\frac{m}{4}-\frac{r}{2}\right)N_2 \end{aligned} \tag{49}$$

where *n, m* and *r* are the number of carbon, hydrogen and oxygen atoms in the fuel molecule, respectively. The variable λ is the excess air factor, which is equal to the reciprocal of equivalence ratio

(also equal to the actual air–fuel ratio divided by the stoichiometric air–fuel ratio), and ε is the mole ratio of nitrogen to oxygen in air. The mole fraction of O_2 in the exhaust stream is [16]

$$x_{O_2} = \frac{\left(\frac{1-f}{f}\right)(n\alpha + m\beta + r\gamma) - n - \frac{m}{4} + \frac{r}{2}}{\left(\frac{1-f}{f}\right)(n\alpha + m\beta + r\gamma)(\epsilon + 1) + \frac{m}{4} + \frac{r}{2}} \tag{50}$$

where f is called the mixture fraction defined by

$$f = \frac{\dot{m}_{fuel}}{\dot{m}_{fuel} + \dot{m}_{air}} = \frac{1}{1 + AFR} \tag{51}$$

and the excess air factor λ is defined by

$$\lambda = \left(\frac{1-f}{f}\right)\frac{n\alpha + m\beta + r\gamma}{n + \frac{m}{4} - \frac{r}{2}} \tag{52}$$

where α, β and γ are constants defined as

$$\alpha = \frac{a_C}{2a_O + 2\varepsilon a_N}, \quad \beta = \frac{a_H}{2a_O + 2\varepsilon a_N}, \quad \gamma = \frac{a_O}{2a_O + 2\varepsilon a_N}$$

with a_c, a_H, a_o and a_N representing the atomic masses of carbon, hydrogen, oxygen and nitrogen, respectively. The interested reader is referred to [16] for more details. From (50), x_{O_2} is a function of *AFR*

$$x_{O_2} = k\left(\frac{1-f}{f}\right) \tag{53}$$

where k is a scalar function and from (51) and (53) we have

$$x_{O_2} = k(AFR) \tag{54}$$

As an approximation, the first three terms of the Taylor series expansion of function $k(.)$ is retained as:

$$x_{O_2} = c_1 AFR^2 + c_2 AFR + c_3 \tag{55}$$

The comparison between the actual oxygen content in the exhaust stream and the estimation from (55) is shown in Fig. 16. This figure demonstrates that the quadratic approximation in (55) for oxygen flow in the exhaust stream is very close to its actual value, and this simple quadratic approximation will make the biodiesel blend estimation computationally more attractive.

Fig. 17 illustrates the parameter variation vectors for different biodiesel blends. From this figure, estimation is accomplished based on the first coefficient which belongs to the regressor AFR^2. This estimator is as follows

$$BD = 200.2\left(c_{2,B0}^{O2} - c_2\right) + 3.1 \tag{56}$$

where c_2 is calculated from the adaptation of the second term coefficient in the model (55) and $c_{2,B0}^{O2}$ is the coefficient of the first term in (55) for regular diesel and no measurement error condition.

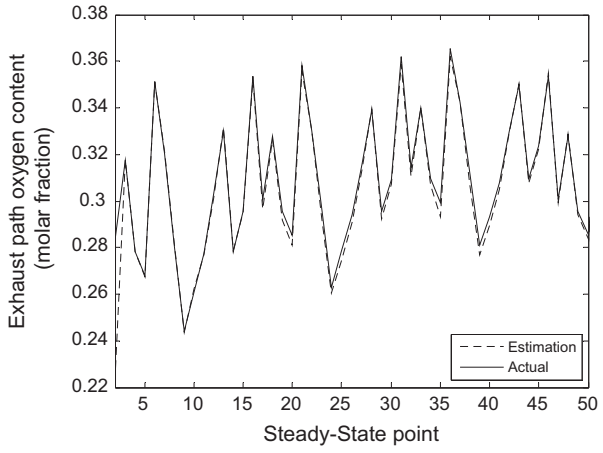

Fig. 16. Oxygen content estimation (for blend *B*50) using {*AFR*} as the regressor.

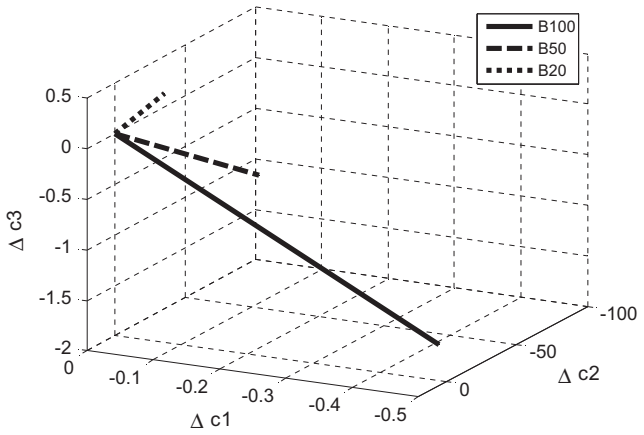

Fig. 17. Parameter variation vectors for different biodiesel blends for oxygen content in exhaust stream.

3.3.2. Sensitivity analysis

Similar to the previous sections, the sensitivity of the designed estimator against measurement error from the sensors and ECU readings is studied. From (56), the partial derivative of the designed estimator in Section 3.3.1 with respect to the second model coefficient is as follows

$$\frac{\partial BD}{\partial c_2} = 200.2 \tag{57}$$

Assuming that in the estimation of *B*50, there is a 2% error in UEGO sensor measurement, then

$$\Delta BD_{O_2\ error} = \Delta c_{2,50} \times \left.\frac{\partial BD}{\partial c_2}\right|_{B50} = 8\% \tag{58}$$

where $\Delta c_{2,50}$ is the deviation of the second coefficient in the presence of measurement error from the coefficients without the effect of measurement errors. The designed estimator is not sensitive to error in UEGO sensor measurement, but it is sensitive to error in *AFR* value. For instance, if there is a 4% error in *AFR* value, then we have

$$\Delta BD_{AFR\ error} = \Delta c_{2,50} \times \left.\frac{\partial BD}{\partial 2}\right|_{B50} = 27\% \tag{59}$$

As can be seen, the error is large compared to the actual blend which is *B*50.

4. Results comparison and discussion

In Section 3, three different approaches for biodiesel blend estimation were developed. The list of the measurements and ECU readings for different approaches are summarized in Table 3. This table shows that the torque-fuel approach and the NO_x sensor-based approach requires three measurements, while the oxygen sensor-based biodiesel blend estimation uses only two measurements. The torque-fuel approach is the only approach that uses a sensor set currently existing on production engines.

The accuracy of the estimation without the effect of measurement errors is almost similar for the different methodologies. The largest estimation error belongs to blend *B*20 among blends {*B*0, *B*20, *B*50, *B*100}. Table 4 shows the maximum absolute estimation error corresponding to different biodiesel blend estimation approaches. From this table, we can see that the NO_x sensor-based approach is the most accurate method followed by the torque-fuel approach and then the UEGO-based method.

Beyond accuracy of the estimation without any measurement error, robustness of the designed estimator against measurement

Table 3
Different measurements and ECU reading required for each biodiesel blend estimation approach.

Method	Adaptive model		
	Input 1	Input 2	Output
Crankshaft torsionals and fuel	Fuel flow rate	Average engine speed	M_6
NO_x sensor	Fuel flow rate	AFR	NO_x sensor
UEGO sensor	AFR	–	UEGO sensor

Table 4
Accuracy of different biodiesel blend estimators.

Method	Max absolute error (%)
NO_x sensor	0.66
Torque-fuel	1.15
UEGO sensor	3.1

errors is very important. Fuel flow rate value, *AFR* value and all the sensor measurements for M_6, NO_x and oxygen are different from the actual values. Therefore, a robustness analysis of the designed estimators is necessary to assess their performance in the presence of measurement errors. For the adaptive estimation approach in Section 3, each estimation method was based on a model whose inputs and output are listed in Table 3. Fuel flow rate, *AFR* and average engine speed are three inputs that are used in all methods. Average engine speed is a more accurate measurement compared to fuel flow rate and *AFR*. Moreover, measurement of M_6 from a Hall-effect sensor, measurement of NO_x emissions from NO_x sensor, and oxygen content measurement of the exhaust path using UEGO sensor are affected by some errors which are inevitable in any measurements.

4.1. Error in fuel flow rate value

Information about fueling rate from ECU can be different from the actual amount of fuel being injected by the injector in the combustion chamber due to control errors of the injection system. Measuring fuel flow rate depends on a lot of factors in the engine, such as injection pressure and the pulse applied to the injector for the injection. In any control system, there would be some error due to error in the actuators and sensors and delay in the feedback. According to [27] the maximum possible error in fuel flow rate measurement considering all of the error factors is ±0.6%. This error value is considered to be ±1% in this paper. For torque-fuel approach, the maximum biodiesel blend estimation error affected by existence of ±1% error in fuel flow rate measurement or estimation is 3.93% which is not very different from the maximum error without any error. The reason is that the length of the parameter variation vector is not changing so much in the presence of ±1% error in fuel flow rate. Hence, the biodiesel estimation error is very small. For the NO_x sensor-based estimation method, the maximum absolute error for biodiesel blend estimation for the same error in fuel flow rate is 0.66%, which is not much different from the accuracy of the estimator. The reason can be explained similarly to the torque-fuel approach. Table 5 summarizes this information.

4.2. Error in air to fuel ratio value

Measuring *AFR* depends on measurement or estimation of $\dot{m}_f$ and $\dot{m}_a$. The relation is

$$AFR = \frac{\dot{m}_a}{\dot{m}_f} \tag{60}$$

Table 5
Maximum absolute error in biodiesel blend estimation in the presence of measurement error in fuel flow rate.

Method	Fuel flow rate error (%)	Max *BD* estimation error (%)
NO_x sensor	±1	0.66
Torque-fuel	±1	1.6

Table 6
Maximum absolute error in biodiesel blend estimation in the presence of measurement error in *AFR*.

Method	*AFR* error (%)	Max. *BD* estimation error (%)
NO_x sensor	±4	0.66
UEGO sensor	±4	27

Then the error in *AFR* value depends on the error in $\dot{m}_f$ and $\dot{m}_a$. The maximum error in $\dot{m}_f$ is considered to be ±1% in Section 4.1, while the maximum error in $\dot{m}_a$ measurement or estimation is reported to be ±4% according to [27]. By some simple calculations, we determine ±4% and ±1.01% error in *AFR* in the presence of ±4% error in $\dot{m}_a$ and ±1% error in $\dot{m}_f$, respectively. Therefore, the maximum possible error in *AFR* is ±4%. The maximum biodiesel blend estimation error affected by this error in *AFR* value is 0.66% and 25.31% for NO_x sensor-based and UEGO sensor based estimation methods, respectively. Table 6 summarizes this information.

4.3. Error in M_6, NO_x and UEGO sensor measurements

Measurements of M_6, NO_x and oxygen content of the exhaust path also have some errors similar to fuel flow rate and *AFR*. For M_6 measurement, it is considered to be affected by up to ±5%. The number is considered to be high, because of the fact that the engine speed signal is needed to go through two filters to provide M_6 value. This error value leads to the maximum error of 3.1% in biodiesel blend estimation for crankshaft torsionals and fuel approach. The maximum error for NO_x measurement is assumed to be ±10% [28]. The reason is that NO_x measurement is affected by oxygen content and other gases in the exhaust path. Therefore, it is considered to be very high. This amount of error leads to the maximum error of 5.9% in biodiesel blend estimation for NO_x sensor-based estimation method. Finally, it is reported to be ±1.5% in [27]. This error is considered to be ±2% in this paper. This error value leads to the maximum error value of 8% in biodiesel blend estimation for UEGO sensor-based estimation approach. The summary of this information is shown in Table 7.

4.4. Estimators performance comparison

In the last section, the effect of different measurement errors on the biodiesel blend estimation error for all the methods is presented. To summarize the information in Tables 4–7, the best achievable performance from each estimator is listed in Table 8.

Table 7
Maximum absolute error in biodiesel blend estimation in the presence of measurement errors.

Method	Measurement	Error value (%)	Max. *BD* estimation error (%)
Torque-fuel	M_6	±5	3.1
NO_x sensor	NO_x	±10	5.9
UEGO sensor	Oxygen	±2	8

Table 8
Performance comparison of different estimators.

Method	Measurement/ estimate	Error value (%)	Min *BD* estimation error (%)	Max *BD* estimation error (%)
Crankshaft torsionals and fuel	$\dot{m}_f$	±1	0.04	1.6
	N	±2	0.04	1.8
	M_6	±5	0.04	3.1
NO_x sensor	$\dot{m}_f$	±1	0.14	0.7
	AFR	±4	0.14	0.7
	NO_x	±10	0.03	5.9
UEGO sensor	*AFR*	±4	0.9	27
	Oxygen	±2	0.5	8

In this table, the accuracy of the estimator in a worst case of the measurement error is also reported.

The maximum error is about 8% for different cases of measurement error existence except for an error in *AFR* value for UEGO sensor-based approach, which is about 27%. Comparing these three estimators in Table 8, we conclude that the crankshaft torsionals and fuel approach is a more reliable method from the following points of view:

- There is no need of adding new sensor(s).
- The method is robust to measurement errors.

5. Conclusion

Different possibilities for biodiesel blend estimation in diesel engines are presented in this paper. The accuracy and robustness of the methods are studied and compared using the data collected from an engine model built in GT-Power. The first proposed approach is based on a torque estimation method, which along with fueling information from ECU results in biodiesel blend estimation. Results from a diesel engine model developed in GT-Power show that this method is very robust against measurement errors. This method has no need of adding a new sensor to the engine. The second method uses the NO_x sensor information for the purpose of biocontent estimation. The fundamental principle of this method is the fact that biodiesel produces more NO_x emissions compared to conventional diesel. This difference in NO_x emissions is the base for biodiesel blend estimation using a NO_x sensor. The method was shown to be very robust, even in the existence of large errors in NO_x sensor measurement. However, the need for a NO_x sensor in the exhaust is a drawback of the method. The last method is based on the measurement from a wide-band oxygen sensor in the exhaust path. This method shows good accuracy, but measurement errors would result in large errors in the biodiesel blend estimation. Hence, this method is less robust compared to the former ones.

References

[1] Murugesan A, Umarani C, Subramanian R, Nedunchezhian N. Bio-diesel as an alternative fuel for diesel engines - A review. Renew Sust Energy Rev 2009;13:653–62.
[2] Basha SA, Gopal KR, Jebaraj S. A review on biodiesel production, combustion, emissions and performance. Renew Sust Energy Rev 2009;13:1628–34.
[3] Tat M, Van Gerpen J. Biodiesel blend estimation using a fuel composition sensor. American Society of Agricultural Eng. 01-6052; 2001.
[4] Hoekman SK. Biofuels in the US – Challenges and opportunities. Renew Energy 2009;34(1):14–22.
[5] E. Van Thuijl, C.J. Roos, L.W.M. Beurskens, An overview of biodiesel technologies, markets and policies in Europe, technical report, Energy Research Centre of the Netherlands, January 2003.
[6] Hossain S, Salleh A, Nasrulhaq Boyce A, Chowdhury P, Naqiuddin M. Biodiesel fuel production from algae as renewable energy. Am J Biochem Biotechnol 2008;4:250–4.
[7] Wu F, Wang J, Chen W, Shuai S. A study on emission performance of a diesel engine fueled with five typical methyl ester biodiesels. Atmos Environ 2009;433:1481–5.
[8] Puhan S, Nagarajan G. NO_x reduction in DI diesel engine using biodiesel as a renewable fuel. Int J Sust Energy 2008;27(3):143–54.
[9] Shahid EM, Jamal Y. A review of biodiesel as vehicular fuel. Renew Sust Energy Rev 2008;12:2484–94.
[10] Canakci M, Van Gerpen JH. Comparison of engine performance and emissions for petroleum diesel fuel, yellow grease biodiesel, and soybean oil biodiesel. American Society of Agricultural Eng. Paper No. 016050; 2001.
[11] Ozsezen AN, Canakci M, Turkcan A, Sayin C. Performance and combustion characteristics of a DI diesel engine fueled with waste palm oil and canola oil methyl esters. Fuel 2009;88:629–36.
[12] Ropkins K, Quinn R, Beebe J, Li H, Daham B, Tate J, et al. Real-world comparison of probe vehicle emissions and fuel consumption using diesel and 5% biodiesel (*B5*) blend. Sci Total Environ 2007;376:267–84.
[13] United States Environmental Protection Agency. A Comprehensive Analysis of Biodiesel Impacts on Exhaust Emissions, Report EPA420-P-02-001, October 2002.
[14] Yuan W, Hansen AC. Computational investigation of the effect of biodiesel fuel properties on diesel engine NO_x emissions. Int J Agric Biol Eng 2009;2(2):41–8.
[15] Hansen AC, Gratton MR, Yuan W. Diesel engine performance and NO_x emissions from oxygenated biofuels and blends with diesel fuel. Trans ASABE 2006;49:589–95.
[16] Snyder DB, Washington EG, Indrajuana AP, Shaver GM. Steady-state biodiesel blend estimation via a wideband oxygen sensor. In: American Control Conference, Seattle, WA, June 2008.
[17] Gamma technology, engine and vehicle simulation (http://www.gtisoft.com).
[18] McCrady J, Hansen A, Lee C. Modeling biodiesel combustion using GT-Power. ASABE Annual International Meeting; 2007.
[19] Franco J, Franchek M, Grigoriadis K. Real-time brake torque estimation for internal combustion engines. Mech Syst Signal Proc 2008;22:338–61.
[20] Heywood JB. Internal Combustion Engines Fundamental. Mc Grow-Hill; 1988.
[21] Mirheidari S, Mohammadpour J, Grigoriadis KM, Franchek MA. Biodiesel blend estimation based on fuel consumption and engine power. In: American control conference, Baltimore, MD, June 2010.
[22] Franchek MA, Buehler PJ, Makki I. Intake air path diagnostics for internal combustion engines. ASME J Dynam Syst Measure Control 2007;129:32–40.
[23] Docquier N, Candel S. Combustion control and sensors: a review. Prog Energ Combust 2002;28:107–50.
[24] Koshizaki N, Oyama T. Sensing characteristics of ZnO-based NO_x sensor. Sensor Actuator 2000;66:119–21.
[25] Yoo J, Chatterjee S, Wachsman ED. sensing properties and selectives of a WO_3/YSZ/Pt potentiometric NO_x sensor. Sensors Actuator 2007;122:644–52.
[26] Brosha EL, Mukundan R, Lujan R, Garzon FH. Mixed potential NO_x sensors using film electrodes and electrolytes for stationary reciprocating engine type application. Sensors Actuator 2006;119:398–408.
[27] Snyder DB, Adi GH, Bunce MP, Satkoski CA, Shaver GM. Fuel blend estimation for fuel-flexible combustion control: uncertainty analysis. Control Eng Pract 2010;18:418–32.
[28] http://www.vdo.fr/generator/www/fr/fr/vdo/main/products_solutions/special_oem_solutions/sensors/download/flc_sv_NOx_sensor_datasheet_en.pdf.
[29] Kegl B. Experimental investigation of optimal timing of the diesel engine injection pump using biodiesel fuel. Energy Fuel 2006;20:1460–70.
[30] Knothe G. Determining the blend level of mixtures of biodiesel with conventional diesel fuel by fiber-optic near infrared spectroscopy and 1H nuclear magnetic resonance spectroscopy. J Am Oil Chem Soc 2001;78:1025–8.
[31] Zawadzki A, Shrestha D, He B. Biodiesel blend level estimation using ultraviolet absorption spectra. Am Soc Agric Biol Eng 2007;50(4):1349–53.
[32] Benjumea P, Agudelo J, Agudelo A. Basic properties of palm oil biodiesel–diesel blends. Fuel 2008;87:2069–75.
[33] Saleh HE. Effect of exhaust gas recirculation on diesel engine nitrogen oxide reduction operating with jojoba methyl ester. Renew Energy 2009;34:2178–86.